# Hyperfine structure of the $(5d+6s)^3$ configuration of $^{139}$La I: New measurements and *ab initio* multiconfigurational Dirac-Fock calculations

W. J. Childs
*Argonne National Laboratory, Argonne, Illinois 60439-4843*

U. Nielsen
*Institute of Physics, University of Aarhus, DK-8000 Aarhus C, Denmark*
(Received 6 April 1987)

The atomic-beam laser-rf double-resonance method has been used to measure precisely the dipole and quadrupole hyperfine structure (hfs) of 11 levels of the $5d^26s$ configuration and four levels of the $5d^3$ configuration of $^{139}$La I. The results, together with earlier results for lower-lying levels, are compared in detail with new multiconfiguration Dirac-Fock (MCDF) *ab initio* calculations. The agreement is good to fair overall, but is poor in some areas. The comparison yields new insights and suggests areas in which the theoretical approach must be improved. In particular, the theory underestimates the importance of contact hfs in the $5d^26s$ configuration by 25–40%. In addition, there is at present no self-consistent way in the MCDF approach to take account of the large core polarization observed in the $5d^3\,^4F$ term.

## I. INTRODUCTION

The study of the structure of the neutral lanthanum atom has a long history; Meggers[1,2] and Russell[2] were among the early contributors. The lowest energy levels,[3] including those studied in the present work, lie in the even-parity configurations $5d6s^2$, $5d^26s$, and $5d^3$. Hyperfine structure (hfs) studies of the $5d6s^2\,^2D_{3/2,5/2}$ levels by Ting[4] in 1957 showed that configuration interaction plays a very important role even in the ground term.

Extension of this work to 11 excited $5d^26s$ levels by Childs and Goodman[5] in 1971 was analyzed by the newly available effective-operator theory of Sandars and Beck.[6] The results indicated that the hfs of the lower-lying $5d^26s$ levels could be a accounted for reasonably well by the parameterized effective-operator approach, but that the hfs of higher $5d^26s$ levels was more difficult to understand. The most extensive effective-operator studies of the hfs of La I were by Ben Ahmed *et al.*[7] High-lying $5d^26s$ levels, for which accurate quadrupole hfs $B$ values are first reported in this paper, are discussed below with reference to this earlier study. Although Bauche-Arnoult[8] has treated in detail how the effects of configuration interaction on hfs can be taken into account by introducing additional (higher-order) parameters, the focus of the present work will be to analyze the La I hfs using *ab initio* calculations.

Within the last two years the multiconfiguration Dirac-Fock (MCDF) theory of Desclaux[9] has been extended by Cheng[10] to allow *ab initio* calculation of the hfs of heavy, many-electron atoms with no adjustable parameters. While it cannot be expected that this approach will either reproduce known hfs splittings or predict new splittings with the precision of the effective-operator approach, one can hope to attain new insights into the complexities of the structure. One can also hope to identify problems or limitations of the MCDF approach itself, as presently formulated, and thereby to encourage further development of the method.

The MCDF method has recently[10–13] been applied to hfs in the $4f$ shell of rare-earth atoms. In the $4f^{12}6s$ configuration of Er II, the calculations[11] were found to underestimate the contribution of contact hfs by about 25%. One goal of the present work is to extend these studies to the $5d$ shell to see if similar trends occur there. To this end precise hfs measurements have been made for the remainder of the levels of the $5d^26s$ configuration in $^{139}$La I. These are supplemented by measurements in the lowest ($^4F$) term of the $5d^3$ configuration. The data now available are of high quality and span most of the generalized configuration $(5d+6s)^3$.

## II. EXPERIMENTAL

This paper describes measurements made on a tightly collimated atomic beam of neutral lanthanum in vacuum. The beam was produced by electron-bombardment heating of a small tantalum oven 1.7 cm high by 0.7 cm diameter. The atoms effused through a 1-mm hole in the top of the oven to form a vertical atomic beam. The beam was studied using both Doppler-free laser-induced fluorescence (LIF) and laser-rf double-resonance spectroscopy. For the LIF studies a weak ($\sim$0.1 mW) "probe" beam from a tunable, single-frequency cw dye laser intersected the atomic beam orthogonally. The fluoresence was collected by an ellipsoidal collector and directed through an interference filter (with a FWHM of 100 Å) to a cooled, photon-counting photomultiplier. The filter greatly reduced background due to photons from the atomic-beam source. For some of the lines studied it was possible to select a fluorescence decay channel different from the excitation channel, so that the

 

filter, in addition, virtually eliminated background from scattered laser photons. The wavelength of the laser was determined to within about ±0.002 Å by an interferometric λ meter using fringe counting. The separations between the hfs components in an optical line were measured with a 50-cm confocal Fabry-Perot etalon. Some of the laser light was passed through the etalon and the fringes observed (at 150-MHz intervals) when the laser was swept provided a convenient standard for measurement of incremental laser frequency.

For the laser-rf double-resonance studies, the weak probe beam described above was supplemented by a strong (~50-mW) "pump" beam of identical wavelength that intersected the atomic beam closer to its source. When the laser was tuned to resonance with an atomic line, the pump beam strongly depleted the population of the lower level of the transition. Under these conditions, the probe beam induced very little fluorescence unless the depleted lower level was repopulated in the space between the two interaction regions. This was achieved by driving an rf transition between the depleted hfs level and a nearby populated level. The Zeeman effect due to the Earth's magnetic field was eliminated by shielding, and the linewidth of such rf transitions was small enough that the hfs spacings in the lower level could be measured with high precision. A PDP-11 computer was used to sweep the rf repetitively, collect the fluorescence data, and determine the centers of the observed resonance curves. The apparatus has been described previously.[14]

Table I lists the atomic lines[15] used in the present study. The wavelength (in air) is given in the first column, and the excitation energies and spectroscopic descriptions of the lower and upper states[3] of the transition are summarized in the next six columns. The central wavelength of the interference filter used in detecting the fluorescence is given in the final column. Although most of the lines studied are listed in Ref. 15, no lines were known in convenient wavelength regions to access some of the levels to be studied. A study of the list of known levels[3] revealed a number of possible allowed lines, however, and of this set those that were observed and used are indicated in Table I with a superscript "b."

Figure 1 shows the hyperfine structure observed in a typical laser scan. The laser was swept slowly through the line at $\lambda = 5874.73$ Å and the fluorescence recorded through a 4100-Å filter. Strong fluorescence from the 24 507.87-$cm^1$ upper level at 4079.18 Å (to the ground state) revealed the 12 hfs components shown. The linewidth (FWHM) of about 20 MHz results primarily from residual Doppler broadening due to imperfect collimation of the atomic beam. By means of the incremental frequency markers (whose positions are shown in the upper abscissa) the separations, together with the known $J$ values (the nuclear spin $I$ is[16] $\frac{7}{2}$ for $^{139}$La) and the stan-

TABLE I. Lines used in the present study of $^{139}$La I. The first column gives the exciting wavelength, and the final column the pass-band filter used for viewing fluorescence. Columns 2 through 7 give identifying data for the lower and upper states of each transition.

| Laser wavelength in air (Å)[a] | Even-parity lower state Configuration | Excitation energy ($cm^{-1}$) | $SLJ$ | Odd-parity upper state Configuration | Excitation energy ($cm^{-1}$) | $J$ | Filter used (Å) |
|---|---|---|---|---|---|---|---|
| 5761.84 | $5d^26s$ | 2668.19 | $^4F_{3/2}$ | $5d6s6p$ | 20 018.99 | $\frac{3}{2}$ | 5300 |
| 5900.75 | $5d^26s$ | 7231.41 | $^4P_{1/2}$ | $4f5d6s$ | 24 173.83 | $\frac{3}{2}$ | 4600 |
| 5874.73 | $5d^26s$ | 7490.52 | $^4P_{3/2}$ | $4f5d6s$ | 24 507.87 | $\frac{5}{2}$ | 4100 |
| 6108.48 | $5d^26s$ | 7679.94 | $^4P_{5/2}$ | $5d^26p$ | 24 046.10 | $\frac{5}{2}$ | 4200 |
| 5823.83 | $5d^26s$ | 8052.16 | $^2F_{7/2}$ | $5d^26p$ | 25 218.27 | $\frac{5}{2}$ | 4100 |
| 5877.99 | $5d^26s$ | 8446.04 | $^2D_{3/2}$ | $5d6s6p$ | 25 453.95 | $\frac{1}{2}$ | 3900 |
| 6032.34[b] | $5d^26s$ | 9044.21 | $^2P_{1/2}$ | $5d^26p$ | 25 616.95 | $\frac{1}{2}$ | 3900 |
| 5827.56 | $5d^26s$ | 9183.80 | $^2D_{5/2}$ | $5d^26p$ | 26 338.93 | $\frac{5}{2}$ | 4000 |
| 6159.39[b] | $5d^26s$ | 9719.44 | $^2P_{3/2}$ | $5d^26p$ | 25 950.32 | $\frac{3}{2}$ | 4000 |
| 5808.06 | $5d^26s$ | 9919.82 | $^2G_{9/2}$ | $5d^26p$ | 27 132.44 | $\frac{7}{2}$ | 5300 |
| 5821.99 | $5d^26s$ | 9960.90 | $^2G_{7/2}$ | $5d^26p$ | 27 132.44 | $\frac{7}{2}$ | 5300 |
| 6072.58[b] | $5d^3$ | 12 430.61 | $^4F_{3/2}$ | $4f5d6s$ | 28 893.51 | $\frac{1}{2}$ | 4600 |
| 5981.07[b] | $5d^3$ | 12 787.40 | $^4F_{5/2}$ | $4f5d6s$ | 29 502.18 | $\frac{5}{2}$ | 3500 |
| 6045.28[b] | $5d^3$ | 13 238.32 | $^4F_{7/2}$ | $4f5d6s$ | 29 775.58 | $\frac{5}{2}$ | 4500 |
| 6191.14[b] | $5d^3$ | 13 747.28 | $^4F_{9/2}$ | $4f5d6s$ | 29 894.91 | $\frac{7}{2}$ | 4500 |

[a]Wavelengths are from Ref. 15 except where noted.
[b]Wavelength not listed in Ref. 15; value cited is obtained from difference of energy levels listed in Ref. 3.

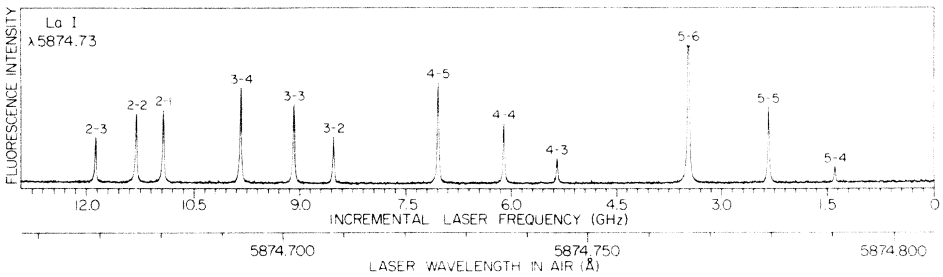


FIG. 1. Spectrum produced by scanning the laser through the hfs components of the line at 5874.73 Å. The linewidth of about 20 MHz includes some residual Doppler broadening. The fluorescence was viewed through a 4100-Å pass-band filter to reduce background, while allowing fluorescence at 4079.18 Å to pass.

dard first-order theory[17] of atomic hyperfine structure, give the values of the magnetic dipole ($A$) and electric quadrupole ($B$) hfs constants for both the lower and upper states of the transition.

Figure 2 shows the appearance of a typical laser-rf double-resonance observation. The transition shown is for the $F=6\leftrightarrow5$ hfs interval in the $^2F_{7/2}$ level at 8052.16 $cm^{-1}$ excitation. The laser was held fixed on the appropriate optical hfs component, thereby depleting the population of the lower state. The resonant increase in fluorescence occurs when the rf scan passes through the frequency corresponding to the $F=6\leftrightarrow5$ hfs splitting. The linewidth (FWHM) of 9 kHz arises from the transit time of the atom in the rf field region, and the hfs interval can be easily determined to ±1 kHz, or about 1 ppm. Although the width observed for such rf transitions can depend on the rf power used, the central (resonance) frequency is insensitive to the power level. Because of the extreme narrowness of such lines it is essential to limit the region through which the rf is scanned in searching for a resonance. This can be done by making use of the relatively crude (±1 MHz) values of the hfs intervals obtained from the LIF scans, as described above.

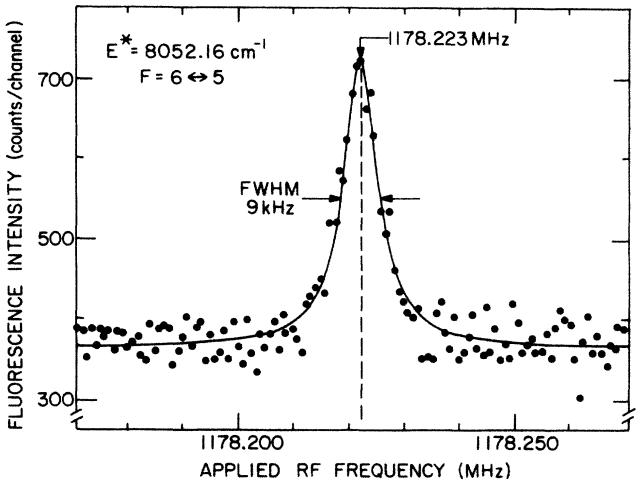


FIG. 2. Double-resonance signal corresponding to the $F=6\rightarrow5$ transition in the $^2F_{7/2}$ level at 8052.16 $cm^{-1}$. The 95% resonant increase in fluorescence has a linewidth of 9 kHz, determined by the flight time of the atoms through the rf region.

## III. SUMMARY OF RESULTS

Table II lists the hfs constants determined for $^{139}$La by laser-induced fluorescence. The first three columns specify the excitation energy, configuration, and the $S$, $L$, and $J$ values of the state, and the hfs constants are given in the final two columns. The uncertainties are typically ±0.5 MHz for the $A$ values and ±4 MHz for the $B$ values. The hfs constants are given below for many of the same levels to much higher precision, as determined from the double-resonance studies.

Table III lists the values of the zero-field hyperfine intervals as determined by laser-rf double resonance. The uncertainty in the observed intervals is 1–2 kHz for those up to 5 GHz, and 2–4 kHz for the larger intervals. The first two columns give the excitation energy and $J$ value of the level, and the third column gives the $F$ values between which the hfs interval is measured. The final two columns give the $A$ and $B$ values that result from fitting the observed intervals using the simple two-parameter first-order hfs theory (magnetic octupole and higher-order interactions are ignored). Corrections for second-order hfs interactions[17] (i.e., hfs interactions with other atomic states) have not been included. Because the electric quadrupole moment $Q$ in $^{139}$La is relatively small, the magnetic dipole hfs interaction is much larger than the electric quadrupole interaction. More specifically, the second-order dipole hfs interaction is entirely comparable with the first-order electric quadrupole interaction. Thus the error in the $B$ values uncorrected for second-order effects may be considerable.

The present results for the $5d^3$ configuration are the only measurements available for the $B$ values (radio-frequency precision is in fact essential for obtaining quantitative quadrupole hfs information). The present results also include the first $B$ values reported for many levels of the $5d^26s$ configurations. In addition, the present $A$ values are much more precise than previous measurements.

The present results supplement earlier studies, both optical and radiofrequency, of the hfs of $^{139}$La. The previous rf studies,[4,5] carried out with the atomic-beam magnetic-resonance method, yielded precise $A$ and $B$ values for most of the $^{139}$La levels up to about 7500 $cm^{-1}$; these results are not included in Table III which lists only the present results, mostly for more highly excited levels. Precise hfs measurements have now been

made for all known[3] atomic levels of $^{139}$La I below 16 500 $cm^{-1}$ excitation.

## IV. INTERPRETATION AND COMPARISON WITH THEORY

The two lowest levels in neutral lanthanum are the $^2D_{3/2,5/2}$ levels of the $5d6s^2$ configuration. It is well known[18] that the hfs of these levels, like that of the corresponding levels in $^{175}$Lu I,[19] cannot be understood on the basis of a single-configuration model. The simple, one-configuration theory[17] predicts $A(^2D_{3/2})/A(^2D_{5/2})=2.33$ and $B(^2D_{3/2})/B(^2D_{5/2})=0.700$, while the measured values in $^{139}$La I are 0.775 and 0.826, respectively. As discussed below, the single-configuration approach is also inconsistent with the observed hfs of many high-lying metastable levels in $^{139}La$ I.

### A. Semiempirical effective-operator approach

The semiempirical effective-operator approach has been applied in detail[7] to study the fine and hyperfine structure of lanthanum. The approach is to choose a basis space, and to evaluate the radial integrals of the Coulomb and spin-orbit interactions within this space by iteratively least-squares fitting the theoretical eigenvalue differences to the appropriate known excitation energies of the atom. With the eigenvectors that result, one then evaluates the hfs in first-order perturbation theory. The radial integrals in the effective-operator hfs Hamiltonian are treated as adjustable parameters in fits to the observed hfs constants. The most complete work of this kind on $^{139}$La, by Ben Ahmed *et al.*,[7] selected as a basis the states of $(5d+6s)^3$, which included the three lowest-lying $L$-$S$ configurations $5d6s^2$, $5d^26s$, and $5d^3$. Because this study was so complete, we make no new calculations of this type. In particular, we consider how the present measurements, especially the newly measured $B$ values

TABLE II. Hfs constants determined for $^{139}$La I by Doppler-free laser fluorescence. The uncertainties are ±0.5 MHz for the $A$ values and ±4 MHz for the $B$ values.

| Excitation energy ($cm^{-1}$) | Configuration | $SLJ$ | hfs constants (MHz) $A$ | $B$ |
|---|---|---|---|---|
| 2668.19 | $5d^26s$ | $^4F_{3/2}$ | −480.6 | 14.1 |
| 7490.52 | $5d^26s$ | $^4P_{3/2}$ | 931.0 | 37.6 |
| 7679.94 | $5d^26s$ | $^4P_{5/2}$ | 802.0 | −36.9 |
| 8052.16 | $5d^26s$ | $^2F_{7/2}$ | −197.3 | 39.4 |
| 8446.04 | $5d^26s$ | $^2D_{3/2}$ | −422.5 | −7.2 |
| 9044.21 | $5d^26s$ | $^2P_{1/2}$ | 226.8 | 0. |
| 9183.80 | $5d^26s$ | $^2D_{5/2}$ | 876.6 | −0.6 |
| 9719.44 | $5d^26s$ | $^2P_{3/2}$ | −655.3 | −32.6 |
| 9919.82 | $5d^26s$ | $^2G_{9/2}$ | 560.3 | 196.6 |
| 9960.90 | $5d^26s$ | $^2G_{7/2}$ | −292.4 | 66.2 |
| 12 430.61 | $5d^3$ | $^4F_{3/2}$ | 445.5 | −17.1 |
| 12 787.40 | $5d^3$ | $^4F_{5/2}$ | 98.4 | −29.8 |
| 13 238.32 | $5d^3$ | $^4F_{7/2}$ | −19.3 | −15.9 |
| 13 747.28 | $5d^3$ | $^4F_{9/2}$ | −63.8 | −26.2 |
| 20 018.99 | $5d6s6p$ | $J=\frac{3}{2}$ | −41.1 | 1.8 |
| 24 046.10 | $5d^26p$ | $^4D^0_{5/2}$ | 327.8 | −36.3 |
| 24 173.83 | $4f5d6s$ | $^4F^0_{3/2}$ | −228.2 | 0.5 |
| 24 507.87 | $4f5d6s$ | $^4F^0_{5/2}$ | 187.3 | 6.2 |
| 25 218.27 | $5d^26p$ | $J=\frac{5}{2}$ | 100.7 | 24.9 |
| 25 453.95 | $5d6s6p$ | $J=\frac{1}{2}$ | −385.1 | 0 |
| 25 616.95 | $5d^26p$ | $^4P^0_{1/2}$ | −296.8 | 0 |
| 25 950.32 | $5d^26p$ | $J=\frac{3}{2}$ | 479.2 | 10.1 |
| 26 338.93 | $5d^26p$ | $^4P^0_{5/2}$ | 100.7 | −5.6 |
| 27 132.44 | $5d^26p$ | $^2G^0_{7/2}$ | 75.8 | 45.0 |
| 28 893.51 | $4f5d6s$ | $^4D^0_{1/2}$ | −455.9 | 0 |
| 29 502.18 | $4f5d6s$ | $J=\frac{5}{2}$ | 50.2 | −8.4 |
| 29 775.58 | $4f5d6s$ | $J=\frac{5}{2}$ | 470.2 | −3.0 |
| 29 894.91 | $4f5d6s$ | $J=\frac{7}{2}$ | 468.5 | −0.5 |

TABLE III. Hfs intervals measured by laser-rf double resonance for metastable levels of $^{139}$La I. The uncertainties are 1–2 KHz for frequencies below 5 GHz, and 2–4 kHz for those above 5 GHz. The hfs constants given in the last two columns result from least-squares fitting the two-parameter first-order hfs theory to the observed intervals. No uncertainties are given for these "observed" hfs constants since they have not been corrected for second-order hfs. These effects are substantial for some of the $B$ values and are discussed in detail in the text.

| Excitation energy ($cm^{-1}$) | $J$ | $F \leftrightarrow F'$ | Hyperfine structure (MHz) Observed hfs interval | $A$ | $B$ |
|---|---|---|---|---|---|
| 2668.19 | $\frac{3}{2}$ | 5↔4 | −2390.615 | −480.292 | 15.188 |
| | | 4↔3 | −1925.506 | | |
| | | 3↔2 | −1451.728 | | |
| 7231.41 | $\frac{1}{2}$ | 4↔3 | 9840.644 | 2460.161 | 0 |
| 7490.52 | $\frac{3}{2}$ | 5↔4 | 4674.682 | 929.618 | 37.221 |
| | | 4↔3 | 3707.825 | | |
| | | 3↔2 | 2762.278 | | |
| 7679.94 | $\frac{5}{2}$ | 6↔5 | 4795.439 | 802.172 | −34.186 |
| | | 5↔4 | 4009.667 | | |
| | | 3↔2 | 2417.501 | | |
| | | 2↔1 | 1614.096 | | |
| 8052.16 | $\frac{7}{2}$ | 7↔6 | −1361.981 | −197.064 | 40.754 |
| | | 6↔5 | −1178.223 | | |
| | | 5↔4 | −989.476 | | |
| | | 4↔3 | −796.573 | | |
| | | 3↔2 | −600.341 | | |
| 8446.04 | $\frac{3}{2}$ | 5↔4 | −2116.822 | −422.399 | −6.753 |
| | | 4↔3 | −1687.663 | | |
| | | 3↔2 | −1262.378 | | |
| 9044.21 | $\frac{1}{2}$ | 4↔3 | 907.569 | 226.892 | 0 |
| 9183.80 | $\frac{5}{2}$ | 6↔5 | 5256.493 | 876.319 | −2.772 |
| | | 5↔4 | 4381.492 | | |
| | | 4↔3 | 3505.908 | | |
| | | 3↔2 | 2629.855 | | |
| | | 2↔1 | 1753.431 | | |
| 9719.44 | $\frac{3}{2}$ | 5↔4 | −3299.435 | −655.138 | −33.249 |
| | | 4↔3 | −2611.058 | | |
| | | 3↔2 | −1941.658 | | |
| 9919.82 | $\frac{9}{2}$ | 8↔7 | 4555.752 | 559.812 | 202.638 |
| | | 7↔6 | 3943.948 | | |
| | | 6↔5 | 3349.169 | | |
| | | 5↔4 | 2768.920 | | |
| | | 4↔3 | 2200.726 | | |
| 9960.90 | $\frac{7}{2}$ | 7↔6 | −2016.965 | −292.267 | 67.537 |
| | | 6↔5 | −1746.669 | | |
| | | 5↔4 | −1468.190 | | |
| | | 4↔3 | −1182.851 | | |
| | | 3↔2 | −891.992 | | |
| | | 2↔1 | −596.977 | | |
| | | 1↔0 | −299.185 | | |
| 12430.61 | $\frac{3}{2}$ | 5↔4 | 2213.952 | 445.086 | −16.068 |
| | | 4↔3 | 1784.934 | | |
| 12787.40 | $\frac{5}{2}$ | 6↔5 | 576.565 | 97.510 | −16.521 |
| | | 5↔4 | 486.956 | | |
| | | 4↔3 | 393.815 | | |
| | | 3↔2 | 297.843 | | |
| 13238.32 | $\frac{7}{2}$ | 7↔6 | −142.677 | −19.103 | −20.898 |
| | | 6↔5 | −116.751 | | |
| | | 5↔4 | −93.382 | | |

TABLE III. (*Continued*).

| Excitation energy ($cm^{-1}$) | $J$ | $F \leftrightarrow F'$ | Hyperfine structure (MHz) Observed hfs interval | $A$ | $B$ |
|---|---|---|---|---|---|
| 13 747.28 | $\frac{9}{2}$ | 8↔7 | −521.066 | −63.829 | −27.385 |
| | | 7↔6 | −450.228 | | |
| | | 6↔5 | −381.671 | | |
| | | 5↔4 | −315.071 | | |
| | | 4↔3 | −250.101 | | |

of a number of $5d^26s$ and $5d^3$ levels fit in with the previous analysis.

For the two lowest levels of *La* I, nominally $5d6s^2\,{}^2D_{3/2,5/2}$, even the multiconfiguration treatment described gave very poor agreement with the measured hfs, and a greatly expanded basis was used[7] in an attempt to understand the low $^2D$ states. With the addition of the configurations $4f6s6p$, $5d^27s$, and $5d6s7s$, the fit was improved but still not good.

For the levels nominally in the $5d^26s$ configuration, reasonably accurate $A$ values were available for the analysis of Ben Ahmed *et al.*,[7] and the present precise values will not affect their conclusions appreciably. The dipole hfs is dominated by the contact contribution of the 6*s* electron. Ben Ahmed *et al.* had relatively few accurate $B$ values to work with, however, and we have made a new fit to the complete set of precise $B$ values using her eigenvectors. When the new $B$ values are added to the data set, the quadrupole radial hyperfine parameter $b_{5d}$ assumes the value $b_{5d}=115(5)$ MHz. Although the fit (one parameter fitting 13 $5d^26s$ $B$ values) contains some scatter, this is much reduced when the effects of second-order hfs are included. These are especially important for the $^2G_{7/2,9/2}$ levels (which lie only 42 $cm^{-1}$ apart), and for the $^4P$ levels.

Some important information is obtained in carrying out the second-order corrections. Because the quadrupole hfs is extremely small, the perturbation of a particular hfs level $F$ of $^2G_{7/2}$ by the hfs level of the same $F$ in the nearby $^2G_{9/2}$ state is closely proportional to

$$\frac{|\langle {}^2G_{7/2},F\,|\,H(M-1)\,|\,{}^2G_{9/2},F\rangle|^2}{E({}^2G_{7/2})-E({}^2G_{9/2})} \propto \frac{(a_{5d}^{01}-a_{6s})^2}{\Delta E}\ .$$

Since $a_{6s} \gg a_{5d}$, the perturbation is nearly proportional to $(a_{6s})^2$, and the radial hfs integral $a_{6s}$ can be determined by the requirement that the second-order corrections must change the $B$ values of the $^2G$ levels by the right amounts to make them consistent with the analysis of the $B$ values of the other $5d^26s$ levels (which are nearly unaffected by second-order effects). This procedure yields a value of $a_{6s}$ of about 4300 MHz, consistent with the value obtained by Ben Ahmed *et al.*[7] from consideration of the first-oder magnetic dipole hfs.

In the treatment of Ben Ahmed *et al.*[7] the eigenvectors for the $5d^3\,{}^4F$ levels contain an explicit contribution from the 6*s* electron because of the inclusion of the $5d^26s$ configuration in the basis set. The contribution of the 6*s* electron to the contact hfs of the $5d^3\,{}^4F$ states is small, however, and a fit to the $A$ values is not very sensitive to the value used for $a_{6s}$. It is found, on the other hand, that the contactlike contribution associated with the 5*d* electron is extremely large and contributes more to the dipole hfs of the $^4F$ levels than the parameters $a_{5d}^{01}$ or $a_{5d}^{12}$. If we require $a_{5d}^{01}=a_{5d}^{12}$ and fix $a_{6s}=4299$ MHz (as determined in Ref. 7), we find

$$a_{5d}^{01}=122\pm2 \text{ MHz}\ ,$$

$$a_{5d}^{10}=-464\pm15 \text{ MHz}\ .$$

Although the Sandars and Beck[6] relativistic effective-operator theory of hfs predicts that $a_{5d}^{10}$ is not zero, the value −464 MHz is more than an order of magnitude larger than is reasonable for a 5*d* electron. The dipole hfs clearly has a strong contact part, but it cannot arise directly from the 5*d* electron shell and does not appear to be due to the 6*s* electron. It presumably arises from configuration interaction with configurations containing unclosed *s* shells. These are very likely inner shells, and core polarization[20–22] (distortion of closed, inner *s* shells) is probably responsible for the large contact hfs. Although the value of $a_{5d}^{10}$ is held equal to zero in the treatment of Ben Ahmed *et al.*,[7] an earlier study[5] that allowed this parameter to vary found $a_{5d}^{10}=-170$ MHz in the $5d6s^2$ configuration. When this is compared with Ben Ahmed's result $a_{5d}^{10}=-261$ MHz for $5d^26s$ and the present result −464 MHz for $5d^3$, we see that $a_{5d}^{10}$ appears to be proportional to the number of 5*d* electrons in the open shell. This suggests rather strongly a core-polarization-related origin for the large contact hfs in the $5d^3$ levels. This problem will be discussed further below using the MCDF *ab initio* approach.

In fitting the newly available quadrupole hfs constants of the $5d^3\,{}^4F$ levels, only the parameter $b_{5d}$ is required for a good fit and we find $b_{5d}=109\pm11$ MHz. This result is essentially unchanged by inclusion of the relativistic parameters $b^{11}$ and $b^{13}$. The value found for $b_{5d}$ is not significantly different from the result of 115 MHz reported above for the $5d^26s$ levels. Second-order effects are not significant for the $^4F$ levels of the $5d^3$ configuration.

### B. Multiconfiguration Dirac-Fock (*ab initio*) treatment

Although the effective-operator formalism of Sandars and Beck[6] allows one to represent much experimental data in terms of a few fundamental parameters, the inherent problem of this approach remains the lack of detailed understanding of the interactions responsible for the observed hfs. The proper way to achieve this goal of understanding is to employ an *ab initio* procedure to calculate the hfs of each state under consideration. This does not necessarily result in a major improvement of understanding, but even in this case, the cause of our lack of understanding may be deduced from the discrepancies between experiment and *ab initio* values. In this section we discuss application of the MCDF scheme to *ab initio* calculation of $A$ and $B$ for all observed states.

The framework behind hfs calculation of hyperfine coupling constants is described comprehensively in Ref. 10. The basic principles are as follows. Within a certain manifold of basis configurations, eigenstates for the many-electron Dirac Hamiltonian are obtained using a self-consistent procedure. These eigenstates are characterized by total electronic quantum number $J$ and parity. The identification of a particular state is done in terms of its energy, $g$ value, and hyperfine coupling constants. All of these observables can be calculated as soon as the Dirac wave function has been determined.[10] Cheng[10] has written angular recoupling programs allowing an expansion of the theoretical $A$ and $B$ values in the reduced radial parameters of the Sandars-Beck[6] theory, providing for direct comparison with the semiempirical analysis.

The manifold used in our calculations is spanned by the $L$-$S$ configurations $5d6s^2$, $5d^26s$, and $5d^3$. Only for the four levels of the $5d^3\,{}^4F$ term was the basis reduced to $5d^3$. For each state, $A$ and $B$ values are expressed in the form

$$A=\sum C_{k_sk_1}\langle r^{-3}\rangle_{5d}^{k_sk_1}+C_s\langle r^{-3}\rangle_{6s}^{10}C\ ,$$
$$B=\sum C_{k_sk_1}\langle r^{-3}\rangle_{5d}^{k_sk_1}\ , \qquad (1)$$

where all terms are evaluated *ab initio*. The scaling constant $C$ is identically 1 in a pure *ab initio* calculation. As discussed below, certain problems remain with the MCDF scheme when considering open $s$ shells. In this case, $C$ can be assigned a (semiempirical) value consistent with observations.

It should be noted that since the basis sets chosen for the present MCDF calculation do not involve breaking closed inner $s$ shells, any core-polarization effects of this type will not be predicted theoretically, and any failure of the MCDF calculations may consequently arise in part from such omissions. As discussed further below, it is not feasible to include such effects explicitly in the MCDF framework at the present time.

In Table IV, observed and calculated $A$ values for all levels below 14 000 $cm^{-1}$ are listed. The calculated

TABLE IV. Comparison of observed $A$ values with *ab initio* MCDF values. The calculated values reflect no arbitrariness whatever except that of selecting the basis set. The choice was to include the configurations $5d6s^2$, $5d^26s$, and $5d^3$ for all except the four highest-lying levels (those nominally described as $5d^3\,{}^4F_J$); for those four levels, the basis was reduced to the single $5d^3$ configuration. The comparison between theory and experiment is discussed at length in the text.

| | | $A$ value[a] (MHz) | |
|---|---|---|---|
| Level ($cm^{-1}$) | Designation | $A$ (observed) | $A$ (MCDF) |
| 0.000 | $5d6s^2\,{}^2D_{3/2}$ | 141.1959[b] | 111.23 |
| 1053.164 | $5d6s^2\,{}^2D_{5/2}$ | 182.1706[b] | 235.64 |
| 2668.188 | $5d^26s\,{}^4F_{3/2}$ | −480.292 | −398.55 |
| 3010.002 | $5d^26s\,{}^4F_{5/2}$ | 300.563[c] | 250.19 |
| 3494.526 | $5d^26s\,{}^4F_{7/2}$ | 462.868[c] | 392.78 |
| 4121.572 | $5d^26s\,{}^4F_{9/2}$ | 489.534[c] | 451.32 |
| 7011.909 | $5d^26s\,{}^2F_{5/2}$ | 304.372[c] | 271.92 |
| 8052.162 | $5d^26s\,{}^2F_{7/2}$ | −197.064 | −12.80 |
| 7231.407 | $5d^26s\,{}^4P_{1/2}$ | 2460.161 | 1913.46 |
| 7490.521 | $5d^26s\,{}^4P_{3/2}$ | 929.618 | 844.26 |
| 7679.939 | $5d^26s\,{}^4P_{5/2}$ | 802.172 | 731.87 |
| 8446.044 | $5d^26s\,{}^2D_{3/2}$ | −422.399 | −321.39 |
| 9183.797 | $5d^26s\,{}^2D_{5/2}$ | 876.319 | 575.10 |
| 9044.214 | $5d^26s\,{}^2P_{1/2}$ | 226.892 | 111.84 |
| 9719.439 | $5d^26s\,{}^2P_{3/2}$ | −655.138 | −188.96 |
| 9919.821 | $5d^26s\,{}^2G_{9/2}$ | 559.812 | 431.58 |
| 9960.904 | $5d^26s\,{}^2G_{7/2}$ | −292.267 | −178.47 |
| 12 430.609 | $5d^3\,{}^4F_{3/2}$ | 445.086 | 176.15 |
| 12 787.404 | $5d^3\,{}^4F_{5/2}$ | 97.510 | 105.89 |
| 13 238.323 | $5d^3\,{}^4F_{7/2}$ | −19.103 | 86.06 |
| 13 747.276 | $5d^3\,{}^4F_{9/2}$ | −63.829 | 82.06 |

[a]Present work except where noted.
[b]Reference 4.
[c]Reference 5.

values are with no adjustments (i.e., $C=1$). As can be readily seen from Table IV, overall agreement between theory and experiment is of qualitative nature at most. For the $5d6s^2$ and $5d^26s$ levels, the agreement can be somewhat improved by an increase of $C$ in Eq. (1), but even after least-squares adjustment to match experiment, resulting in $C=1.25$, it is observed that agreement still remains poor. One of the main causes for this behavior seems to be due to core polarization. This is especially clear when considering the $5d^3\,^4F$ levels, where there is not even qualitative agreement between theory and experiment. As noted above in discussing the semiempirical model, however, polarization is often included by allowing the contact strength to be a free parameter. If we make a least-squares adjustment of MCDF $A$ values for the $5d^3$ levels to experiment, $\langle r^{-3}\rangle_{5d}^{10}$ being the free parameter, *quantitative* agreement is obtained. The reduced radial parameter thus obtained has a magnitude much larger than the MCDF theoretical value (i.e., that for $C=1$) indicating substantial $s$-electron hfs, presumably due to core polarization. This is a general observation for systems showing core polarization: The contact parameter for non-$s$ electrons often acquires an unexpectedly large value when treated as a free parameter in an effective-operator approach. A fully satisfactory bridge between the description of core polarization (CP) in the MCDF scheme and the outlined free-parameter adjustment procedure remains to be found. Apart from the effect of CP and the problems associated with unpaired $s$ electrons, it is very likely that some major key configurations are missing in the manifold basis, presumably configurations involving $4f$ electrons due to the proximity between the $5d$- and $4f$-shell one-electron energies.

Table V displays observed, corrected, and MCDF $B$ values for all levels observed. Observed and MCDF have the same meaning as in the discussion of $A$ values above. The corrected $B$'s result from the observed $B$'s after second-order hyperfine structure has been taken into account. The framework for obtaining second-order corrections within the MCDF scheme has been described by Cheng *et al.*[23] in the case of $Li^-$. Here we apply the formalism to hfs in a complex spectrum.

The $5d6s^2$ levels are not at all well understood. There is no apparent explanation of the disagreement between experiment and theory. This is in marked contrast to the $5d^26s$ levels, where fair agreement with experiment is achieved for most levels. For some levels they are far off, however, most notably for the $^2G$ levels. These levels are very close energetically, and substantial second-order hfs corrections are expected, and should therefore be carried out before a detailed comparison is made. When this correction is applied using matrix elements calculated purely *ab initio* ($C=1$), the corrections are too small to give agreement with experiment, consistent with the fact that $C=1$ underestimated the contact hfs

TABLE V. Comparison of observed $B$ values with *ab initio* MCDF values. Because of substantial second-order hfs, the observed values (column 3) must be corrected for these perturbations (column 4) before they are compared with the calculated values. The corrections (which are made using the MCDF method), the *ab initio* $B$ values, and the comparison of the latter with experiment are discussed in detail in the text.

| Level ($cm^{-1}$) | Designation | $B$ value (MHz)[a] $B$ (observed) | $B$ (corrected) | $B$ (MCDF) |
|---|---|---|---|---|
| 0.000 | $5d6s^2\,^2D_{3/2}$ | 44.781[b] | | 29.59 |
| 1053.164 | $5d6s^2\,^2D_{5/2}$ | 54.213[b] | | 32.21 |
| 2668.188 | $5d^26s\,^4F_{3/2}$ | 15.188 | 16.348 | 14.84 |
| 3010.002 | $5d^26s\,^4F_{5/2}$ | 10.873[c] | 7.800 | 11.41 |
| 3494.526 | $5d^26s\,^4F_{7/2}$ | 17.925[c] | 16.102 | 15.45 |
| 4121.572 | $5d^26s\,^4F_{9/2}$ | 32.180[c] | 31.535 | 26.17 |
| 7011.909 | $5d^26s\,^2F_{5/2}$ | 28.091[c] | 28.289 | 20.04 |
| 8052.162 | $5d^26s\,^2F_{7/2}$ | 40.754 | 40.349 | 29.02 |
| 7231.407 | $5d^26s\,^4P_{1/2}$ | 0 | 0 | 0 |
| 7490.521 | $5d^26s\,^4P_{3/2}$ | 37.221 | 34.723 | 28.58 |
| 7679.939 | $5d^26s\,^4F_{5/2}$ | −34.186 | −36.365 | −36.09 |
| 8446.044 | $5d^26s\,^2D_{3/2}$ | −6.753 | −6.006 | −0.85 |
| 9183.797 | $5d^26s\,^2D_{5/2}$ | −2.772 | −5.404 | 2.51 |
| 9044.214 | $5d^26s\,^2P_{1/2}$ | 0 | 0 | 0 |
| 9719.439 | $5d^26s\,^2P_{3/2}$ | −33.249 | −33.539 | −22.16 |
| 9919.821 | $5d^26s\,^2G_{9/2}$ | 202.638 | 127.571 | 85.78 |
| 9960.904 | $5d^26s\,^2G_{7/2}$ | 67.537 | 111.512 | 76.66 |
| 12 430.609 | $5d^3\,^4F_{3/2}$ | −16.068 | | −12.02 |
| 12 787.404 | $5d^3\,^4F_{5/2}$ | −16.521 | | −12.91 |
| 13 238.323 | $5d^3\,^4F_{7/2}$ | −20.898 | | −17.80 |
| 13 747.276 | $5d^3\,^4F_{9/2}$ | −27.385 | | −23.87 |

[a]Present work except where noted.
[b]Reference 4.
[c]Reference 5.

to fit the $A$ values.

Several possible ways exist to increase the MCDF second-order corrections, all depending on increasing the contact hfs, i.e., making $C > 1$.

(i) One can adjust $C$ so the $^2G$ levels agree with experiment (for the $B$ values) as these two levels are the most sensitive to second-order interactions. We find very different and large values of $C$ are required for the two $^2G$ levels, indicating that this is a poor way to evaluate $C$. The inability to carry through this approach indicates that some problems which are not understood regarding the $^2G$ term exist.

(ii) We have tried $C=1.25$ as determined from the least-squares fitting in the dipole case. The resulting $B$ values still appear too small, and this procedure is troubled by the lack of understanding of CP for the $A$ values as well as the fact that agreement between experiment and MCDF theory is not very good.

(iii) Finally, we have chosen $C$ to obtain maximum self-consistency between the corrected experimental $^2G$ $B$ values and the $B$'s of all the other $5d^26s$ levels according to the detailed effective-operator treatment.[7] This procedure results in $C=1.40$. All values appearing in the $B$ (corrected) column of Table V have been obtained using this $C$ value. Not very surprisingly, the effect of the second-order corrections is largest for the $^2G$ levels. It is surprising, however, that agreement between experiment and theory for these two states remains poor, in light of overall fair agreement for most of the remaining $5d^26s$ states. The cause of this is not at all understood at the present time.

For the $5d^3$ levels, agreement between experiment and theory is rather good, and no second-order corrections have been carried out for this configuration. This is in sharp contrast to what was found for the dipole hfs, where core polarization is large.

## V. CONCLUSION

For the $5d6s^2$ configuration, neither the semiempirical effective-operator (EO) nor the multiconfiguration Dirac-Fock (MCDF) approach has quantitative success in accounting for either the dipole or quadrupole hfs. The $J$ dependence of the hfs constants is, however, predicted very much better by the MCDF approach than by the single-configuration (pure $5d6s^2$) approach.

For the $5d^26s$ configuration, both the EO and MCDF approaches are disappointing. The predicted hfs, with either approach, is closer to experiment if the size of the contact interaction is adjusted empirically. For the MCDF, an increase of 25–40 % over the *ab initio* value is required. This discrepancy is not understood; it may arise from underestimating the contribution of the $6s$ electron, or from core polarization, or both. For the quadrupole constants, the size of the contact interaction is vital in evaluating the second-order corrections which are very large, especially for the $^2G$ levels. For the $5d^3$ configuration, the effects of core polarization (on the dipole hfs) are entirely comparable to those of the $5d$ electron shell, and it is not yet possible to take account of these in a self-consistent way with the MCDF method.

In summary, we find the results of applying the MCDF theory to the hfs of La I to be disappointing but extremely interesting because of the following.

(1) The MCDF approach tends to underestimate the extent of contact hfs in configurations that contain an unpaired $s$ electron, like $5d^26s$. This is consistent with results just reported for the $4f^{12}6s$ configuration of Er II by Nielson *et al.*[11]

(2) There is no self-consistent way of taking the effects of core polarization on atomic hfs into account using the MCDF approach. Both problems, but especially the second, call for new theoretical effort.

## ACKNOWLEDGMENTS

One of us (U.N.) wishes to acknowledge support from the Danish Natural Science Research Council. This research was supported by the U.S. Department of Energy (Basic Energy Sciences Program), under Contract No. W-31-109-Eng-38.

[1]W. F. Meggers, Bur. Stand. J. Res. **9**, 239 (1932).
[2]H. N. Russell and W. F. Meggers, Bur. Stand. J. Res. **9**, 625 (1932).
[3]*Atomic Energy Levels, The Rare-Earth Elements,* Natl. Bur. Stand. Ref. Data Ser., Natl. Bur. Stand. (U.S.) Circ. No. 60, edited by W. C. Martin, R. Zalubas, and L. Hagen (U.S. GPO, Washington, D.C., 1978).
[4]Y. Ting, Phys. Rev. **108**, 295 (1957).
[5]W. J. Childs and L. S. Goodman, Phys. Rev. A **3**, 25 (1971).
[6]P. G. H. Sandars and J. Beck, Proc. R. Soc. London, Ser. A **289**, 97 (1965).
[7]Z. Ben Ahmed, C. Bauche-Arnoult, and J. F. Wyart, Physica **77**, 148 (1974); Z. Ben Ahmed, J. Verges, M. Wilson, and A. Giacchetti, Physica C **84**, 275 (1976).
[8]C. Bauche-Arnoult, Proc. R. Soc. London, Ser. A **322**, 361 (1971); J. Phys. (Paris) **34**, 301 (1973).
[9]J. P. Desclaux, Comput. Phys. Commun. **9**, 31 (1974).
[10]K. T. Cheng and W. J. Childs, Phys. Rev. A **31**, 2775 (1985).
[11]U. Nielsen, K. T. Cheng, H. Ludvigsen, and J. N. Xiao, Phys. Scr. **34**, 776 (1986).
[12]H. Bruggemeyer, V. Pfeufer, U. Nielsen, and J. F. Wyart, Z. Phys. D **1**, 269 (1986).
[13]W. J. Childs, L. S. Goodman, and K. T. Cheng, Phys. Rev. A **33**, 1469 (1986).
[14]W. J. Childs, O. Poulsen, and L. S. Goodman, Phys. Rev. A **19**, 160 (1979).
[15]*Tables of Spectral-Line Intensities, Arranged by Elements,* Natl. Bur. Stand. (U.S.) Monograph No. 145, edited by W. F. Meggers, C. H. Corliss, and B. F. Scribner (U.S. GPO, Washington, D.C., 1975).
[16]G. H. Fuller, J. Phys. Chem. Ref. Data **5**, 835 (1976).
[17]W. J. Childs, Case Stud. At. Phys. **3**, 215 (1973).
[18]B. G. Wybourne, *Spectroscopic Properties of Rare Earths* (Wiley, New York, 1965), p. 151.
[19]G. J. Ritter, Phys. Rev. **126**, 240 (1962).
[20]A. J. Freeman and R. E. Watson, Phys. Rev. **131**, 2566

(1963); **123**, 2027 (1961).
[21]U. Nielsen, L.-U. Aaen Andersen, O. Poulsen, and E. Riis, J. Phys. B **20**, 1697 (1987).
[22]I. Lindgren and J. Morrison, *Atomic Many-Body Theory* (Springer-Verlag, New York, 1982), p. 346.
[23]K. T. Cheng, J. E. Hardis, E. J. Dehm, and D. R. Beck, Phys. Rev. A **30**, 698 (1984).